Symmetry breaking of nematic umbilical defects through an amplitude equation

Marcel G. Clerc* and Estefania Vidal-Henriquez
Departamento de Física, Facultad de Ciencias Físicas y Matemáticas, Universidad de Chile, Casilla 487-3, Santiago, Chile

Juan Diego Davila and Michał Kowalczyk
Departamento de Ingeniería Matemática and CMM, Universidad de Chile, Casilla 170 Correo 3, Santiago, Chile
(Received 23 April 2014; published 18 July 2014)

The existence, stability properties, and bifurcation diagram of the nematic umbilical defects is studied. Close to the Fréedericksz transition of nematic liquid crystals with negative anisotropic dielectric constant and homeotropic anchoring, an anisotropic Ginzburg-Landau equation for the amplitude of the tilt of the director away from the vertical axis is derived by taking the three-dimensional (3D) to 2D limit of the Frank-Oseen model. The anisotropic Ginzburg-Landau equation allows us to reveal the mechanism of symmetry breaking of nematic umbilical defects. The positive defect is fully characterized as a function of the anisotropy, while the negative defect is characterized perturbatively. Numerical simulations show quite good agreement with the analytical results.

DOI: 10.1103/PhysRevE.90.012507 PACS number(s): 61.30.Jf, 05.45.−a

I. INTRODUCTION

Macroscopic systems with injection and dissipation of energy and momenta exhibit instabilities leading to spontaneous symmetry breaking and pattern formation [1]. Due to the inherent fluctuations of these macroscopic systems, different organizations may emerge in distinct regions of the same sample; hence, spatial structures are usually characterized by domains, separated by interfaces, as grain boundaries, defects, or dislocations [2,3]. Among others, defects in rotationally invariant two-dimensional (2D) systems, i.e., vortices, attract a great deal of attention because of their universal character, as they are solutions of the complex Ginzburg-Landau equation (CGLE) that describes such different systems as fluids, superfluids, superconductors, liquid crystals, fluidized anisotropic granular matter, magnetic media, and optical dielectrics, to mention a few [4]. Vortices occur in complex fields and can be identified as topological defects, that is, pointlike singularities, which locally break the symmetry. They exhibit a zero intensity at the singular point with a phase spiraling around it. The topological charge is assigned by counting the number of spiral arms in the phase distribution, while the sign is given by the sense of the spiral rotation.

Nematic liquid crystals with negative anisotropic dielectric constant and homeotropic anchoring are a natural physical context where dissipative vortices are observed [5,6]. Figure 1 shows the typically observed vortices and schematic representations in two and three dimensions of these defects. Umbilical defects in nematic liquid crystals have long been reported in the literature (see textbooks [5–7] and references therein). Two types of stable vortices with opposite charges are observed [see Fig. 1(c)], which are characterized by being attracted (repulsed) to the opposite (identical) topological charge. The nematic liquid crystal phase is characterized by rod-shaped molecules that have no positional order but tend to point in the same direction. Then, the description of the nematic liquid crystal is given by a vector—the director $\vec{n}$—which accounts for the molecular order. Note that the defects observed in this context are strongly dissipative, compared to those observed in magnetic systems, superfluids, superconductors, and Bose-Einstein condensates. Even so, the vortexlike defects have accompanied liquid crystals since their discovery in 1889 by Lemman [8], who called these structures kernels. Later, they were observed in a similar experimental setup by Freidel, who called these defects *noyaux* [9]. Moreover, he also resolved their detailed topological structure. From the theory of elasticity of nematics liquid crystals Frank calculated the detailed structure of these defects [10]. Due to the fact that these defects break the orientational order and by analogy with dislocations in crystals of condensed matter, Frank called these defects disclinations. Despite the different names given to the observed vortices in this context, none of them were adopted by the community of liquid crystals. There the most widely used name for these defects is nematic umbilical defects. The term umbilics was coined by Rapini [11] and refers to the topological structure of the defect, which corresponds to a stringlike object in three dimensions [see Fig. 1(b)]. Because of the complex elasticity theory associated with nematic liquid crystals, characterized by three types of deformation (blend, twist, and splay), the dynamic study of defects is a thorny task [5–7]. A simple and universal strategy to study and characterize these defects and their dynamics is to analyze their behavior near the orientational instability of the molecules, which is called Fréedericksz transition [5,6]. Close to this transition the dynamics of the director can be reduced at main order to the Ginzburg-Landau equation with real coefficients [12,13]. This amplitude equation allows us to understand the emergence of different orientational domains, two types of stable vortices, and their respective dynamics. Since the vortices have a $\pm 2\pi$ phase jump (winding number), usually they are referred to as vortex $+$ and $-$, respectively. In this approach, however, both defects are indistinguishable in their amplitude and, as a result of the phase invariance of the Ginzburg-Landau equation, they account for a continuous family of solutions, characterized by a phase parameter. Notwithstanding, as a result of the inherent anisotropy of liquid crystals these defects can be distinguished experimentally.

*marcel@dfi.uchile.cl

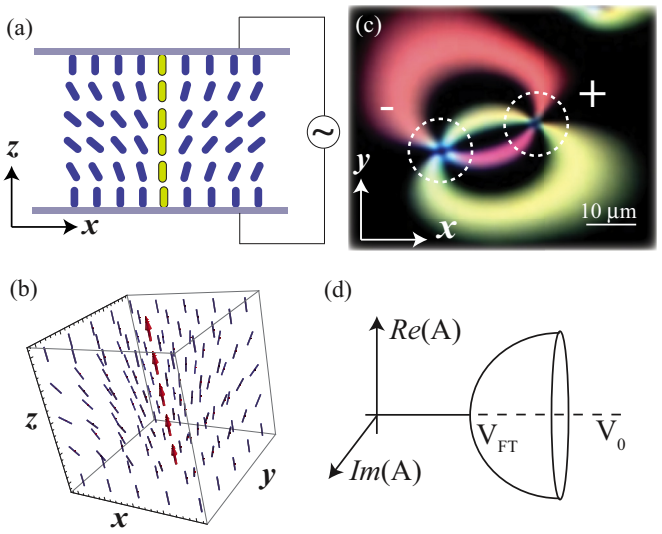

FIG. 1. (Color online) Nematic umbilical defects. (a) Schematic representation of the system under study, the rods describe the orientation of the director and the gray rods (green rods) stand for the vortex position. (b) Three-dimensional representation of the nematic umbilical defect, where arrows stand for the position of the defect. (c) Experimental image of umbilical defects. (d) Bifurcation diagram of a degenerate pitchfork bifurcation with $O(2)$ symmetry.

Figure 1(c) shows an image obtained using two crossed polarizers where one can distinguish between different defects, in which one exhibits a variety of different colors.

The aim of this manuscript is to investigate the existence, stability properties, and bifurcation diagram of the nematic umbilical defects through amplitude equations. Several studies have been performed using variational methods in the free energy of Frank [11,14], however there is no complete characterization of the nematic umbilical defects. Close to the Fréedericksz transition of nematic liquid crystals with negative anisotropic dielectric constant and homeotropic anchoring, an anisotropic Ginzburg-Landau equation for the transversal critical mode is derived by taking the 3D to 2D limit of the Frank-Oseen model. This model allows us to reveal the mechanism of symmetry breaking of nematic umbilical defects. The defect with positive charge is fully characterized as a function of the anisotropy, while the negative defect is characterized perturbatively. In particular, only a discrete number of solutions of the continuous family of defect persists when anisotropy is taken into account.

II. AMPLITUDE EQUATION CLOSE TO THE FRÉEDERICKSZ TRANSITION

Let us consider a nematic liquid crystal layer with negative anisotropic dielectric constant and homeotropic anchoring under the influence of high-frequency electrical tension (kHz). Figure 1(a) shows schematically the liquid crystal layer, where the rods account for the orientation of the director $\vec{n}(\mathbf{r},t)$ and $\{\mathbf{r},t\}$ describe the space and time, respectively. To understand the dynamical behavior of umbilical defects, we derive a model in the vicinity of the Fréedericksz transition, a limit where analytical results are accessible as nematic liquid crystal molecules are weakly tilted from the longitudinal axis $\hat{z}$ and backflow effects can safely be neglected. The dynamical equation for the molecular director $\vec{n}$ reads (the Frank-Oseen model) [6]

$$\begin{aligned}\gamma\partial_t\vec{n} = {} & K_3[\nabla^2\vec{n} - \vec{n}(\vec{n}\cdot\nabla^2\vec{n})] \\ & + (K_3 - K_1)[\vec{n}(\vec{n}\cdot\vec{\nabla})(\vec{\nabla}\cdot\vec{n}) - \vec{\nabla}(\vec{\nabla}\cdot\vec{n})] \\ & + (K_2 - K_3)[2(\vec{n}\cdot\vec{\nabla}\times\vec{n})(\vec{n}(\vec{n}\cdot\vec{\nabla}\times\vec{n}) - \vec{\nabla}\times\vec{n}) \\ & + \vec{n}\times\vec{\nabla}(\vec{n}\cdot\vec{\nabla}\times\vec{n})] + \epsilon_a(\vec{n}\cdot\vec{E})[\vec{E} - \vec{n}(\vec{n}\cdot\vec{E})], \quad (1)\end{aligned}$$

where γ is the relaxation time, ϵ_a is the anisotropic dielectric constant that accounts for nonlinear response of the dielectric constant, $\{K_1,K_2,K_3\}$ are the nematic liquid crystal elastic constants, which account for the elastic deformation of splay, twist, and bend type, respectively. The electric field is given by $\vec{E} = (V/d)\hat{z} \equiv E_z\hat{z}$, where E_z is the root mean square amplitude of the electric field, V is the applied voltage and d is the width of the liquid crystal layer.

A. Amplitude equation close to Fréedericksz transition

A trivial equilibrium of the liquid crystal layer is the homeotropic state, $\vec{n} = \hat{z}$. This state undergoes a degenerate stationary instability when the anisotropic dielectric constant is negative ($\epsilon_a < 0$) for critical values of the voltage, which match the Fréedericksz transition threshold $V_{FT} = \sqrt{-K_3\pi^2/\epsilon_a}$. Then, the director undergoes orientational instability, i.e., the molecules do not want to align with the electric field. As a result of elastic coupling between the molecules, the director has a cone of possible equilibria. From the point of view of bifurcation theory, this instability corresponds to a degenerate pitchfork bifurcation with $O(2)$ symmetry [3]. Figure 1(d) outlines the bifurcation diagram for this instability.

Close to the transition point, we introduce the ansatz

$$\vec{n} = \begin{pmatrix} n_x(\vec{r},\pi z/d,t) \\ n_y(\vec{r},\pi z/d,t) \\ \sqrt{1-(n_x^2+n_y^2)} \end{pmatrix},$$

with $\vec{r} = (x,y) \in \Omega \subset \mathbb{R}^2$ the transverse coordinates, $z \in (-1/2,1/2)$ and the parameter $d \ll 1$ measures the thickness of the liquid crystal sample (which is conveniently taken to be equal to πd). Now the idea is to take the 3D to 2D limit of Eq. (1) near the Fréedericksz point, or in other words take the limit $d \to 0$. To do this we assume that the voltage has the following expansion

$$V = V_{FT} + d^2V_1 + \cdots, \quad V_1 > 0.$$

We introduce the new variable $\zeta = z/d$ and write the ansatz in a more explicit form

$$\begin{aligned} n_x(\vec{r},\zeta,t) &= d^2u_0(\vec{r},t)\cos(\pi\zeta) + d^4u_1(\vec{r},t)\vartheta(\pi\zeta) + \cdots, \\ n_y(\vec{r},\zeta,t) &= d^2v_0(\vec{r},t)\cos(\pi\zeta) + d^4v_1(\vec{r},t)\vartheta(\pi\zeta) + \cdots, \\ n_z(\vec{r},\zeta,t) &= \sqrt{1-(n_x^2+n_y^2)}, \end{aligned}$$

where $\vartheta(\pi\zeta)$ is a function to be determined. Next, we substitute these expressions in Eq. (1) and compare terms with equal powers of d. This allows us to have a hierarchy of equations. It turns out that the $\mathcal{O}(1)$ term in the direction of

the vector $\hat{x} = (1,0,0)$ satisfies

$$K_3 d^{-2}\partial^2_{\zeta\zeta} n_x + \epsilon_a V_{FT}^2 d^{-2} n_x = u_0\left(-K_3\pi^2 - \epsilon_a V_{FT}^2\right) = 0,$$

because of the choice of V_{FT}. Hence, this condition corresponds to impose that the voltage is in the Fréedericksz transition. A similar equation holds in the $\hat{y} = (0,1,0)$ direction. Note that this does not allow us to determine the functions u_0 and v_0. As is the case in the standard formal asymptotic expansion of a homogenization problem, these functions are determined as solvability conditions for the equations corresponding to $\mathcal{O}(d^2)$ order. Indeed, at this order we have to solve, say in the direction of $\hat{x}$, a linear problem for the function ϑ, which is of the form

$$u_1\left[K_3\partial^2_{\zeta\zeta} - \epsilon_a V_{FT}^2\right]\vartheta = g_x(\vec{r},\pi\zeta,t),$$

and this last equation can be solved uniquely if

$$\int_{-1/2}^{1/2} g_x(\vec{r},\pi\zeta,t)\cos(\pi\zeta)\,d\zeta = 0.$$

We show in the Appendix that this, and a similar condition in the $\hat{y}$ direction lead to the following equation for the order parameter $w_0 \equiv u_0 + i v_0$:

$$\begin{aligned}\gamma\,\partial_t w_0 = {} & \tfrac{1}{2}(K_1+K_2)\nabla_\perp^2 w_0 + \tfrac{1}{2}(K_1-K_2)\partial^2_{\eta\eta}\bar{w}_0 \\ & - K_3\pi^2 w_0|w_0|^2 - \epsilon_a V_{FT} V_1 w_0, \end{aligned} \tag{2}$$

where $\bar{w}_0$ stands for the complex conjugate of w_0, $\partial_\eta \equiv \partial_x + i\partial_y$ and $\nabla_\perp^2 \equiv \partial_{xx} + \partial_{yy} = \partial_\eta\partial_{\bar{\eta}}$.

We change variables

$$w_0(\vec{r},t) \longmapsto \frac{1}{\pi}\sqrt{\frac{K_1+K_2}{K_3}}\,A[\vec{\rho},(K_1+K_2)t/2\gamma],$$

and let $\delta = (K_1-K_2)/(K_1+K_2)$. Denoting the new time variable by t again we obtain an anisotropic complex Ginzburg-Landau equation:

$$\partial_t A = \mu_0 A - |A|^2 A + \nabla_\perp^2 A + \delta\partial^2_{\eta\eta}\bar{A}, \tag{3}$$

where

$$\mu_0 = \frac{2|\epsilon_a| V_{FT} V_1}{K_1+K_2}$$

is the bifurcation parameter and $\delta \in [-1,1]$ accounts for the elastic anisotropy.

Similar equations were derived before: using the method of amplitude equations for nematic liquid crystals near the Fréedericksz transition [13] (see also [12]), and for modeling self-organization in an array of microtubules interacting via molecular motors in Ref. [15].

Note that Eq. (3) can be rewritten in the form

$$\partial_t A = -\frac{\delta\mathcal{E}}{\delta\bar{A}}, \tag{4}$$

where the free energy is

$$\mathcal{E}(A,\delta) \equiv \int_\Omega dS\left[|\nabla A|^2 + \frac{1}{2}(\mu_0 - |A|^2)^2 + \delta\mathrm{Re}\{(\partial_\eta\overline{A})^2\}\right], \tag{5}$$

where $\Omega \subset \mathbb{R}^2$ is a bounded domain. In other words the time-dependent anisotropic Ginzburg-Landau Eq. (3) is simply a gradient flow of the free energy. Obviously $\mathcal{E}$ is a Lyapunov functional, i.e.,

$$\begin{aligned}\frac{d\mathcal{E}}{dt} &= \int_\Omega ds\left(\frac{\delta\mathcal{E}}{\delta A}\partial_t A + \frac{\delta\mathcal{E}}{\delta\bar{A}}\partial_t\bar{A}\right), \\ &= -2\int_\Omega ds\frac{\delta\mathcal{E}}{\delta A}\frac{\delta\mathcal{E}}{\delta\bar{A}} \le 0. \end{aligned} \tag{6}$$

The trivial equilibria that minimize the free energy are $|A|^2 = \mu_0$. However, as we will see this equation has nontrivial inhomogeneous equilibria.

B. Isotropic limit: Ginzburg-Landau equation

Considering the isotropic limit ($K_1 = K_2 = K_3$), $\delta = 0$, the above model reduces to the well-known complex Ginzburg-Landau equation with real coefficients

$$\partial_t A = \mu_0 A - |A|^2 A + \nabla_\perp^2 A. \tag{7}$$

This model has gathered a great interest by describing several physical systems such as fluids, superfluids, superconductors, liquid crystals, magnetic media, and optical cavity, to mention a few [4]. The main properties of the complex Ginzburg-Landau equation are reported in the review [16]. This equation admits stable dissipative vortex solutions with topological charge ± 1 [2,4]. Figure 2 illustrates the vortex solution with negative topological charge. If one considers polar representation $A = R_v(r)e^{i(m\varphi+\varphi_0)}$, where $m = \pm 1$ is the topological charge, (r,φ) are the polar coordinates in the plane and φ_0 is a continuous parameter that accounts for the phase invariance of the above amplitude Eq. (7). The magnitude $R_v(r)$ satisfies

$$\mu_0 R_v - R_v^3 - \frac{m^2}{r^2}R_v + \frac{1}{r}\frac{dR_v}{dr} + \frac{d^2R_v}{d^2r} = 0. \tag{8}$$

There are no analytical expressions for the defect solutions of this model, which were first observed numerically in Ref. [17]. However, one has the asymptotic behavior

$$R_v(r) \approx \begin{cases} \alpha_m r^{|m|} + \cdots, & r \longrightarrow 0, \\ \sqrt{\mu_0} - \frac{m^2}{2}r^{-2} + \cdots, & r \longrightarrow \infty, \end{cases}$$

where $\alpha_m > 0$ is a constant that depends on μ_0 as well.

By using Padé approximants, one can obtain suitable approximations for the vortices [2]. There is a long history of literature devoted to the rigorous study of vortices in complex Ginzburg-Landau equation (see Ref. [18] and references therein). Note that the equation for the modulus of the amplitude does not depend on the sign of the topological charge. Hence, both vortices are indistinguishable from the point of view of their magnitude.

In order to characterize the arms of the vortex and to allow a comparison with the experimental observations obtained by using cross polarizers, let us introduce the nullcline field $\psi(r,\theta) \equiv \mathrm{Re}(A)\mathrm{Im}(A)$. This auxiliary field becomes zero when the real or imaginary part of A vanishes. Then, the arms and position of the vortex are represented, respectively, by the zero and the intersection of the zero nullcline curves. Figure 2(c) shows the nullcline field obtained by using the above Ginzburg-Landau equation (7). Note that both defects are still indistinguishable (see Fig. 2), however these defects

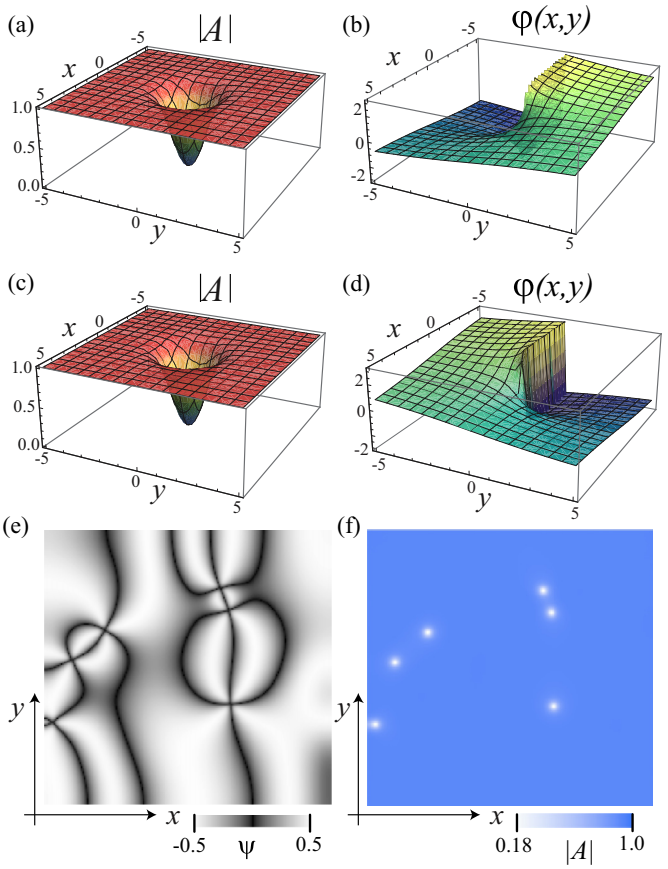

FIG. 2. (Color online) Vortex solution of Ginzburg-Landau equation (7) with $\mu_0 = 1$ (from numerical simulations). Structure of the magnitude (a) and phase of the positive vortex (b). Structure of the magnitude (c) and phase of the negative vortex (d). (e) Nullcline field, $\psi(x,y,t) = \mathrm{Re}(A)\mathrm{Im}(A)$ at given time. This field is equivalent to the light intensity observed when one considers crossed polarizers on an experimental setup. (f) Modulus of the amplitude A at given time.

are experimentally distinguishable [see Fig. 1(c)] [11,14,21]. The different colors observed experimentally are due to the different optical paths produced by the different orientations of the molecules. Moreover, from the Ginzburg-Landau equation, one deduces that the interaction between vortices is symmetric [4,22], however it has been reported that the speed of umbilic defects in the process of collision is different [23]. Numerical simulations considering the dynamic of the nematic liquid crystal show the same result, where the speed asymmetry arises from backflow effects and anisotropy in the elastic constants [23].

The Ginzburg-Landau equation is invariant under the following symmetries: $\vec{r} \longrightarrow \vec{r} + \vec{r}_0$ (spatial translation invariance), $\varphi \longrightarrow \varphi + \varphi_0$ (coordinates rotation), $\varphi \longrightarrow -\varphi$ (coordinates reflection), $A \longrightarrow Ae^{i\varphi_0}$ (phase invariance), and $A \longrightarrow \bar{A}$ (reflection invariance).

III. ANISOTROPY INDUCES SYMMETRY BREAKING

A. Fourfold symmetry of the energy and its consequences

For the purpose of the following discussion we assume that $\mu_0 = 1$. Let us now consider the effect of the anisotropy of the elastic constants ($\delta \neq 0$). From the point of view of symmetries, equation (7) as well as the free energy $\mathcal{E}$ are still invariant under spatial translation, but phase invariance and coordinates rotation are no longer valid symmetries. They are replaced by a joint symmetry $A(z,t) \longrightarrow A(ze^{-i\varphi_0},t)e^{i\varphi_0}$ (z is the complex variable that represents the Cartesian plane). Using the notation $\mathcal{R}_{\varphi_0}$ for the rotation by the angle φ_0 of $\mathbb{R}^2$ about the origin, a short calculation shows however that we still have:

$$\mathcal{E}(A,\delta) = \mathcal{E}(A \circ \mathcal{R}_{\varphi_0}, -\delta) = \mathcal{E}(\mathcal{R}_{\varphi_0} A, -\delta),$$

when $\varphi_0 = \pi/2$. This is best seen if we notice that with $A = u + iv$ we have

$$\mathcal{E}(A,\delta) = \int_\Omega dS[(1+\delta)(u_x + v_y)^2 + (1-\delta)(u_y - v_x)^2] + \frac{1}{4}\int_\Omega dS[1-(u^2+v^2)]^2.$$

We say that $\mathcal{E}$ has a fourfold symmetry in the sense that

$$\mathcal{E}(A,\delta) = \mathcal{E}[\mathcal{R}_{m\pi/2} A \circ \mathcal{R}_{k\pi/2}, (-1)^{m+k}\delta]. \tag{9}$$

This formula relates different equations and energies when $m+k$ is odd, and at the same time it shows that energy and bifurcation diagrams have to be even symmetric with respect to $\delta = 0$. Functionals with fourfold symmetries appear for instance in the so-called d-wave Ginzburg-Landau equation, see for instance Refs. [19,20] and the references therein.

The presence of anisotropy also breaks the symmetry between the vortices with positive and negative charge. To give a first insight into this issue let us suppose that $\Omega = B_L$ is a ball of radius L centered at the origin. Consider a function f defined in Ω with Fourier series expansion

$$f(z) = \sum_{n=-\infty}^{\infty} f_n(r) e^{in\theta},$$

with $z = re^{i\theta}$. Now, if $f(z)$ has the form

$$f(z) = \sum_{n=-\infty}^{\infty} f_{4n\pm1}(r) e^{i(4n\pm1)\theta},$$

that is, only modes indexed by $4n \pm 1$ are present, it can be checked that

$$\Delta u + \delta \partial_{\eta\eta}\bar{u} + u(1-|u|^2)$$

has an expansion where again only modes $4n \pm 1$ appear. With this in mind we can define A to be a vortex solution with unit positive charge if its Fourier series has the terms indexed by $4n+1$ and $f_1'(0) \neq 0$, and unit negative charge if its series has the terms $4n-1$ and $f_{-1}'(0) \neq 0$.

Figure 3 illustrates the vortices with positive and negative topological charge found in the asymmetric Giznburg-Landau equation (3). Note that from the nullcline field $\psi(r,t)$ it is not possible to differentiate these vortices, compared to the magnitude field $|A(r,t)|$ where they are distinguishable (cf. Fig. 3). For the vortex with charge $+1$, the modulus remains rotationally invariant, while for the -1 vortex the rotational invariance around the core is broken by the fourfold symmetry. Indeed, in a single color map representation of $|A|$, one can identify the positive and negative charges on their circular and

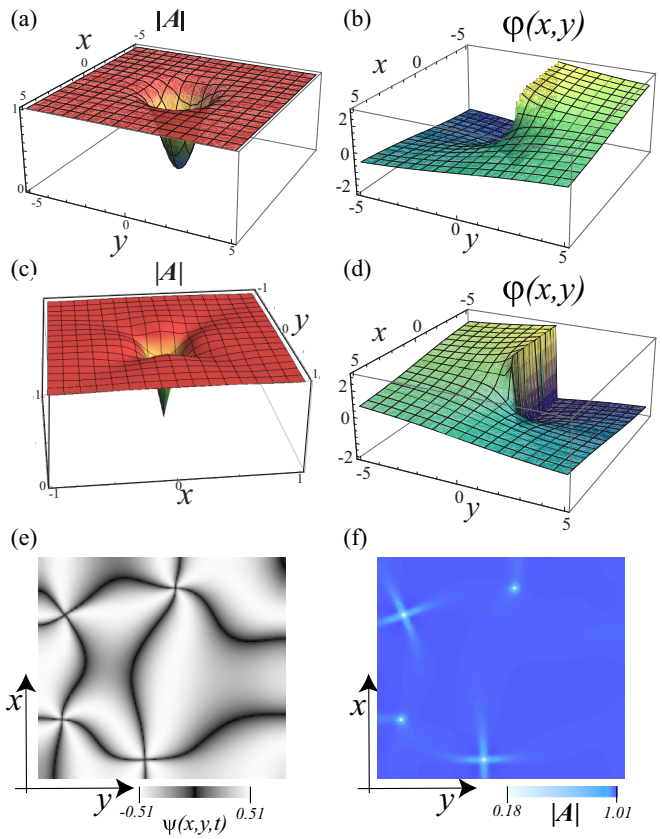

FIG. 3. (Color online) Vortex solution of the anisotropic Ginzburg-Landau equation (3) with $\mu_0 = 1$ and $\delta = 0.7$ (from numerical simulations). Structure of the magnitude (a) and phase of the positive vortex (b). Structure of the magnitude (c) and phase of the negative vortex (d). (e) Colormap of nullcline field $\psi(x,y,t) = \mathrm{Re}(A)\mathrm{Im}(A)$ and (f) modulus of the amplitude A at given time.

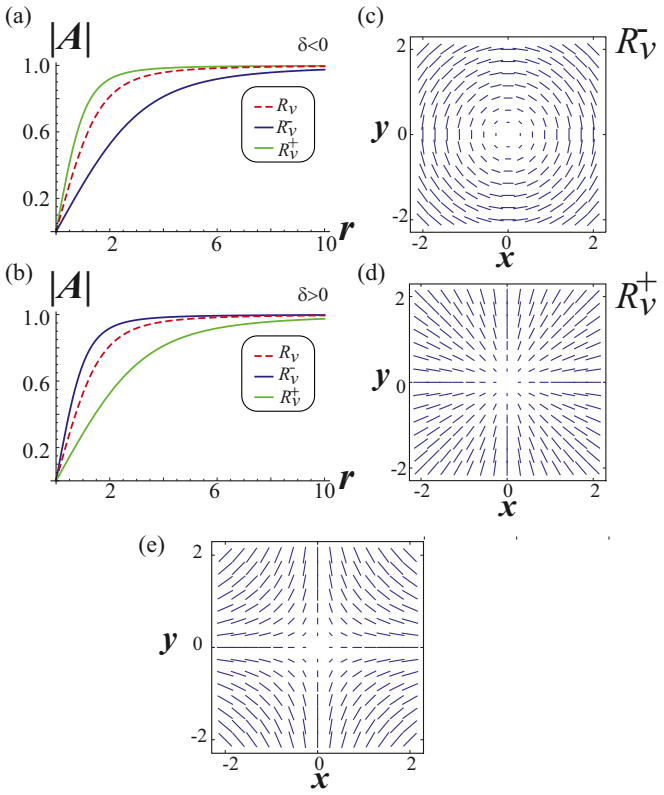

FIG. 4. (Color online) Vortex solution with positive topological charge of the anisotropic Ginzburg-Landau equation (3) with $\mu_0 = 1$ and $\delta = 0.1$. Magnitude of the vortex with positive (a) and negative (b) anisotropy, respectively. The dashed curve stands for the magnitude of the vortex for isotropic systems ($\delta = 0$). (c) and (d) schematic representation of the orientation field $A(r,\theta,\{\varphi_0\})$ for different values of φ_0: R_v^- ($\varphi_0 = \pi/2$) and R_v^+ ($\varphi_0 = 0$). (e) Schematic representation of the orientation amplitude field for the negative topological charge.

cross structure, respectively [cf. Fig. 3(d)]. Note that when one increases the anisotropy, the size of the cross structure grows. Below, we study the properties of each of the vortices.

B. Vortex with positive charge

By introducing the ansatz $A(r,\theta,\{\varphi_0\}) = R(r)e^{i(\theta+\varphi_0)}$ in the anisotropic Ginzburg-Landau equation (3), for the vortex solution with positive topological charge, we obtain the following set of scalar equations

$$0 = \mu_0 R - R^3 + (1+\delta e^{-2i\varphi_0})\left(\frac{d^2R}{d^2r} + \frac{1}{r}\frac{dR}{dr} - \frac{R}{r^2}\right) \quad (10)$$

$$0 = \delta \sin 2\varphi_0 \left(\frac{d^2R}{d^2r} + \frac{1}{r}\frac{dR}{dr} - \frac{R}{r^2}\right). \quad (11)$$

From Eq. (11), the only possibility to obtain a nontrivial solution is to consider the phase parameter satisfying $\sin 2\varphi_0 = 0$, which gives the discrete solutions $\varphi_0 = \{0,\pi/2,\pi,3\pi/2\}$, and which is of course consistent with the fourfold symmetry mentioned above. Therefore, from the continuous family of possible phase jumps only four possibilities survive. On the other hand, the equation for the magnitude of the amplitude reads

$$0 = \mu_0 R - R^3 + (1+\delta\cos 2\varphi_0)\left(\frac{d^2R}{d^2r} + \frac{1}{r}\frac{dR}{dr} - \frac{R}{r^2}\right). \quad (12)$$

Since $\varphi_0 = \{0,\pi/2,\pi,3\pi/2\}$, we must have $\cos 2\varphi_0 = \pm 1$. Rescaling the space by the factor $\sqrt{1\pm\delta}$, the above equation becomes Eq. (8). Therefore, the isotropic positive vortex has the form

$$A = R_v^{\pm}\left(\frac{r}{\sqrt{1\pm\delta}}\right)e^{i(\theta+\frac{\pi}{4}\mp\frac{\pi}{4}+n\pi)}, \quad (13)$$

with R_v the magnitude of the vortex solution of the Ginzburg-Landau equation and $n = 0, \pm 1, \pm 2, \ldots$. Consequently, the anisotropic vortex solution with positive charge corresponds to a simple scaling of the isotropic vortex solution, notwithstanding, with a finite number of possible phase jumps ($\varphi_0 = \{0,\pi/2,\pi,3\pi/2\}$), in opposition, to the isotropic system, which has an infinite number of solutions parameterized by the continuous parameter φ_0. Figure 4 illustrates the magnitude of a vortex with positive topological charge solution for the asymmetric Ginzburg-Landau equation (3), for positive and negative anisotropy. Note that the difference between the

vortices R_v^+ and R_v^- in the amplitude are their different sizes of the vortex core. For positive (negative) anisotropy the largest core is for vortex R_v^+ (R_v^-). Also, due to the different φ_0, both vortices represent different configurations for the director orientation [cf. Figs. 4(c) and 4(d)].

It is worth noting that it is known, from the variational approach to the Frank free energy, that the elastic anisotropy allows a discrete number of four possible phase jumps for umbilical defects with positive topological charge [11,14]. These features are recovered by the analytical expression (13). In the context of self-organization of an array of microtubules interacting via molecular motors similar configurations have been numerically found for the orientational field with $\varphi_0 = 0$ and $\varphi_0 = \pi/2$, which have been denominated, respectively, *aster* and *ideal vortex* [15]. Notice that these configurations and their continuous deformation are vortex solutions like Frank remarked at the dawn of the theory of liquid crystals [10].

C. Free-energy analysis

In order to study the existence, stability properties and bifurcation diagram of the vortex solution with positive topological charge, one can analyze the properties of the free energy $\mathcal{E}$, expression (5). Using the vortex solution $A = R_v^{\pm}(r/\sqrt{1\pm\delta})e^{i(\theta+\varphi_0)}$, where the $\pm$ sign stands for $+$ for $\varphi_0 = \{0,\pi\}$ and $-$ for $\varphi_0 = \{\pi/2,3\pi/2\}$, and taking $\Omega = B_L$ we obtain

$$\mathcal{E} = \pi \int_0^L \left\{ (\partial_r R_v)^2 + \frac{R_v^2}{r^2} + \frac{1}{2}\left(1 - R_v^2\right)^2 + \delta\cos(2\varphi_0)\left(\partial_r R_v + \frac{R_v}{r}\right)^2 \right\} r\,dr, \tag{14}$$

changing variables $\rho = r/\sqrt{1\pm\delta}$, we obtain

$$\mathcal{E} = \pi \int_0^{L/\sqrt{1\pm\delta}} \left\{ (\partial_\rho R_v(\rho))^2 + \frac{R_v^2(\rho)}{\rho^2} + \frac{(1\pm\delta)\left(1 - R_v^2(\rho)\right)^2}{2} \pm \delta\left(\partial_\rho R_v(\rho) + \frac{R_v(\rho)}{\rho}\right)^2 \right\} \rho\,d\rho, \tag{15}$$

after straightforward calculations and following the same strategy presented in Ref. [4], we derive the energy of the vortex with positive topological charge

$$\mathcal{E} = \pi \ln\left(\frac{L}{a_0\sqrt{1\pm\delta}}\right) + \frac{\pi(1\pm\delta)}{2} \pm \pi\delta\left(\ln\left(\frac{L}{a_0\sqrt{1\pm\delta}}\right) + 1\right). \tag{16}$$

Figure 5 shows the energy for the two different vortices with positive topological charge (two respective signs). The lines and geometrical symbols represent, respectively, the energy obtained using formula (16) and obtained from numerical simulations of Eq. (3). The numerical results show quite good agreement with the analytical expressions. Note that this figure shows that the scaling $\sqrt{1\pm\delta}$ that makes the core smaller is the one with less energy and, therefore, preferred by the system. Therefore, if $\delta < 0$ ($\delta > 0$) the solution with minimal energy is the one with $\varphi_0 = \{0,\pi\}$ ($\varphi_0 = \{\pi/2,3\pi/2\}$). Numerical

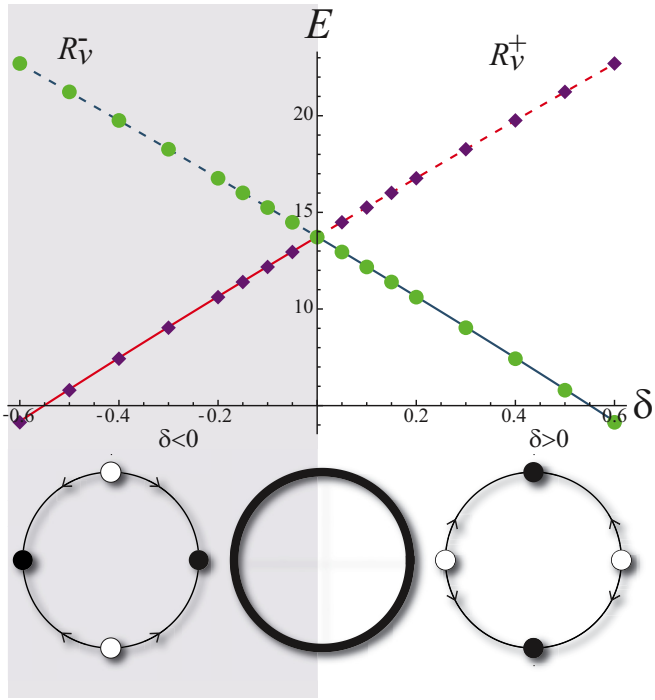

FIG. 5. (Color online) Energy of the positive vortex solutions for different jump phase φ_0 as function of δ. Numerical results obtained from vortex solutions of Eq. (3) are shown by the geometrical symbols (circles and diamonds) and the theoretical result obtained from expression (16) by a continuous and dashed line. The continuous and dashed line indicate, respectively, the stable and unstable vortex solution with positive topological charge. The bottom panel schematically illustrates the bifurcation diagram for the phase jump φ_0, which correspond to a degenerate transcritical bifurcation. The dark and white circles account for stable and unstable vortices solutions.

simulations of the anisotropic Ginzburg-Landau equation (3) show that the vortices with positive topological charge and large core are unstable. Thus, the stable vortices are those with small core. The respective stability of these solutions is represented by continuous (stable) and dashed (unstable) lines in Fig. 5. One expects that vortices with small core are the more stable, because the energy privileges the uniform state $|A|^2 = \mu_0$.

D. Bifurcation diagram

The above analysis shows that there are two positive vortex solutions that exist for every value of δ. These phase singularity solutions exchange stability in the isotropic limit ($\delta = 0$), where $\varphi_0 = \{0,\pi\}$ goes from stable to unstable solution, and vice versa for $\varphi_0 = \{\pi/2,3\pi/2\}$. The mechanism through which these solutions exchange stability is not by the usual collision of solutions of the transcritical bifurcation [24,25], but rather by passing through a very degenerate point at $\delta = 0$, where an infinite number of solutions exist and φ_0 can take any continuous value between 0 and 2π. Hence, this bifurcation is a degenerate transcritical bifurcation and it is schematically shown in the bottom panel in Fig. 5, where the dark and

white circles account for stable and unstable vortex solutions, respectively.

In brief, we have shown that the anisotropic elasticity is responsible for the dissimilarity of the defects with different topological charges. One possible experimental protocol for characterizing several properties of these nematic umbilical defects is through the use of crossed circular polarizers [21] and modification of the elastic constants by changing the temperature. Temperature allows to handle the values of elastic anisotropy constants. In particular, the elastic constants are quite sensitive to temperature near to the nematic-smectic transition [5].

IV. NEGATIVE VORTEX SOLUTION

The above analysis yields a complete description of vortices with topological charge +1. As we have mentioned, in vortices with negative topological charge, their rotational invariance around the core is broken by a fourfold symmetry (see Fig. 3). We will consider the strategy of perturbative analysis of these phase singularity solutions for small anisotropy ($\delta \ll 1$). Hence, we consider the following ansatz

$$A(r,\theta) \approx [R_v(r) + \delta g(r,\theta) + O(\delta^2)]e^{-i[\theta-\delta\Theta(r,\theta)]}, \quad (17)$$

where $g(r,\theta)$ and $\Theta(r,\theta)$ are dominate correction functions to the isotropic negative vortex, and with the condition that Θ has no topological charge, i.e.,

$$\oint_\Gamma \nabla\Theta \cdot d\vec{l} = 0, \quad (18)$$

where the path Γ encircles the core of the vortex. Using the above ansatz (17) in the anisotropic Ginzburg-Landau equation (3) and taking the leading order in δ, we obtain

$$\begin{aligned} 0 = e^{-i\theta}\Bigg[&\mu_0 g - 3R_v^2 g + \frac{\partial^2 g}{\partial r^2} + 2i\frac{\partial\Theta}{\partial r}\frac{\partial R_v}{\partial r} \\ &+ iR_v\frac{\partial^2\Theta}{\partial r^2} + \frac{1}{r}\frac{\partial g}{\partial r} + \frac{iR_v}{r}\frac{\partial\Theta}{\partial r} + \frac{1}{r^2}\frac{\partial^2 g}{\partial\theta^2} \\ &- \frac{2i}{r^2}\frac{\partial g}{\partial\theta} + \frac{iR_v}{r^2}\frac{\partial^2\Theta}{\partial\theta^2} + \frac{2R_v}{r^2}\frac{\partial\Theta}{\partial\theta} - \frac{g}{r^2}\Bigg] \\ &+ e^{3i\theta}\left[\frac{\partial^2 R_v}{\partial r^2} + \frac{3R_v}{r^2} - \frac{3}{r}\frac{\partial R_v}{\partial r}\right], \end{aligned} \quad (19)$$

separating the real and imaginary parts

$$\begin{aligned} 0 = &\mu_0 g - 3R_v^2 g + \frac{\partial^2 g}{\partial r^2} + \frac{1}{r}\frac{\partial g}{\partial r} + \frac{1}{r^2}\frac{\partial^2 g}{\partial\theta^2} + \frac{2R_v}{r^2}\frac{\partial\Theta}{\partial\theta} \\ &- \frac{g}{r^2} + \cos(4\theta)\left[\frac{\partial^2 R_v}{\partial r^2} + \frac{3R_v}{r^2} - \frac{3}{r}\frac{\partial R_v}{\partial r}\right], \end{aligned} \quad (20)$$

$$\begin{aligned} 0 = &2\frac{\partial\Theta}{\partial r}\frac{\partial R_v}{\partial r} + R_v\frac{\partial^2\Theta}{\partial r^2} + \frac{R_v}{r}\frac{\partial\Theta}{\partial r} + \frac{R_v}{r^2}\frac{\partial^2\Theta}{\partial\theta^2} \\ &- \frac{2}{r^2}\frac{\partial g}{\partial\theta} + \sin(4\theta)\left[\frac{\partial^2 R_v}{\partial r^2} + \frac{3R_v}{r^2} - \frac{3}{r}\frac{\partial R_v}{\partial r}\right]. \end{aligned} \quad (21)$$

The θ dependence is easily addressed doing variable separation, by setting $g(r,\theta) = g_4(r)\cos(4\theta)$ and $\Theta(r,\theta) = \theta_4(r)\sin(4\theta)$. Thus we obtain the following set of equations

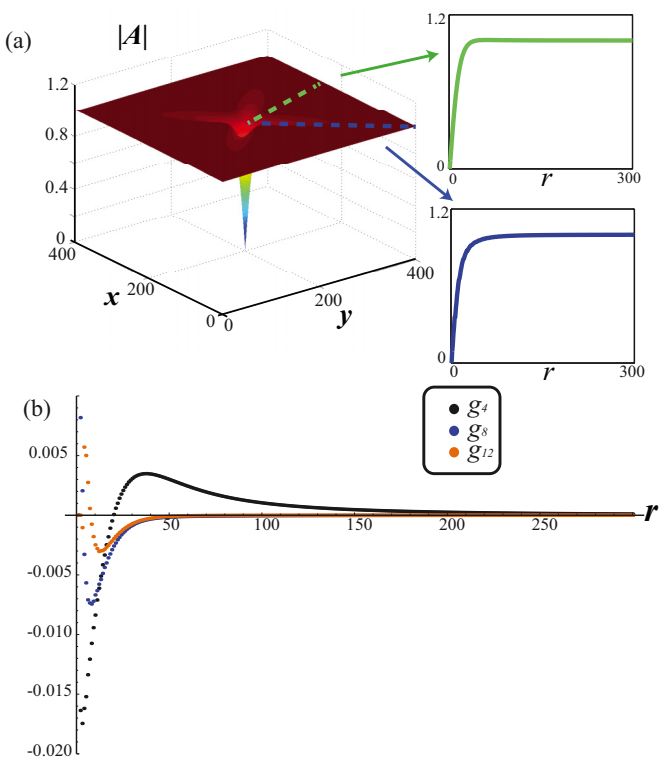

FIG. 6. (Color online) Vortex solution with negative topological charge of anisotropic Ginzburg-Landau equation (3) with $\mu_0 = 1$ and $\delta = 0.7$. (a) left panel magnitude of amplitude $|A|$ and right panels different radial profiles. (b) Numerical coefficients of the modal expansion (25).

for the radial dependency

$$\begin{aligned} 0 = &\mu_0 g_4 - 3R_v^2 g_4 + \frac{\partial^2 g_4}{\partial r^2} + \frac{1}{r}\frac{\partial g_4}{\partial r} - \frac{16 g_4}{r^2} \\ &+ \frac{8R_v\theta_4}{r^2} - \frac{g_4}{r^2} + \frac{\partial^2 R_v}{\partial r^2} + \frac{3R_v}{r^2} - \frac{3}{r}\frac{\partial R_v}{\partial r}, \end{aligned} \quad (22)$$

$$\begin{aligned} 0 = &2\frac{\partial\theta_4}{\partial r}\frac{\partial R_v}{\partial r} + R_v\frac{\partial^2\theta_4}{\partial r^2} + \frac{R_v}{r}\frac{\partial\theta_4}{\partial r} + \frac{8g_4}{r^2} \\ &- \frac{16R_v\theta_4}{r^2} + \frac{\partial^2 R_v}{\partial r^2} + \frac{3R_v}{r^2} - \frac{3}{r}\frac{\partial R_v}{\partial r}. \end{aligned} \quad (23)$$

As $r \to \infty$, the solution of this set of equations behaves as follows

$$g_4(r) \to \frac{9}{4r^2}, \quad \theta_4(r) \to \frac{3}{16}. \quad (24)$$

Then, the phase correction converges to a constant value. Using a variational approach to the Frank free energy far from the core of the vortex, neglecting the spatial dependence, and considering a modal angular expansion, one can recover the value of $\theta_4 = 3/16$ and $g_4 = 0$ [14]. However, this ansatz does not allow us to characterize the spatial structure of the negative vortex solution.

Asymptotically, the correction of the magnitude of the amplitude, $g_4(r)$, decreases as the inverse of the square of the distance. A numerical solution for $g_4(r)$ is shown in Fig. 6, which has quite good agreement with the above asymptotic expression. The magnitude of the amplitude of

the phase singularity with negative topological charge as a function of the radial distance is not monotonous. However, this nonmonotonous feature is weak even for large δ [cf. Fig. 6(a)]. In order to investigate the spatial structure of the magnitude of the amplitude, we have considered the following modal angular expansion

$$|A(r,\theta)| = \sum_{n=2} g_n(r)\cos(n\theta), \tag{25}$$

where $g_n(r)$ are the coefficients of the expansion. Numerically, we have computed the coefficients for the expansion. Figure 6(b) shows some of these coefficients. One expects the mode $g_4(r)$ to be the dominant one even for larger δ as can be seen in Fig. 6(b). Hence, this mode is responsible for the fourfold symmetry of the vortex solutions with negative charge.

Note that in the perturbative analysis the phase jump, φ_0, is not predetermined, because if we consider a more general ansatz

$$A(r,\theta,\varphi_0) \approx [R_v(r) + \delta g(r,\theta)]e^{-i[\theta+\varphi_0-\delta\Theta(r,\theta)]}, \tag{26}$$

the previous analysis remains the same by setting $g(r,\theta) = g_4(r)\cos(4\theta + 4\varphi_0)$ and $\Theta(r,\theta) = \theta_4(r)\sin(4\theta + 4\varphi_0)$. Therefore, the vortex solution with negative topological charge is parametrized continuously by φ_0. Furthermore, when the anisotropy parameter δ is modified numerically, the vortex does not exhibit any bifurcation. Using the vortex solution with negative topological charge obtained numerically from the anisotropic Ginzburg-Landau equation (3) and evaluating the free energy $\mathcal{E}$, formula (5), we can reveal the dependence of the free energy as a function of the anisotropy, $\mathcal{E}(\delta)$. Figure 7 shows this function for various critical points of $\mathcal{E}$. The first observation we make is that the graph of the set $[\delta,\mathcal{E}(\delta)]$ is even. This is a general fact that follows immediately from the relation (9) with $m = 1$ and $k = 0$.

Second, the energy of the vortex with negative charge is exactly alike with the positive one only at $\delta = 0$. The vortex with positive topological charge is always more stable for

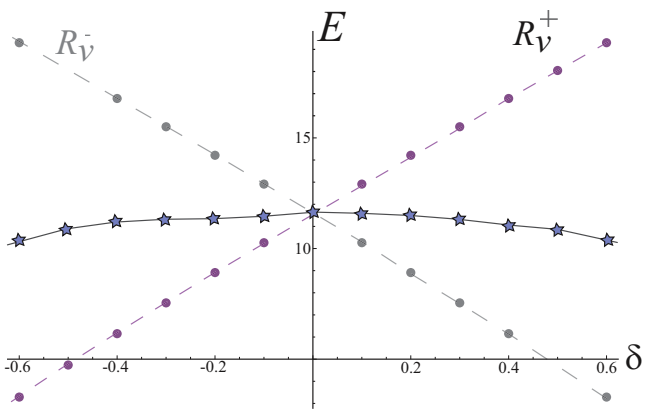

FIG. 7. (Color online) Energy of the vortex solutions as function of δ. The star symbols account for the free energy $\mathcal{E}$ obtained numerically using a vortex with negative topological charge and formula (5). The solid and dashed lines, drawn to guide the eye, show the evolution of the free energy of the vortices with topological negative and positive charge, respectively, as function of the anisotropy.

anisotropic nematic liquid crystals. It is worthy to note that the vortices are always created by pairs to conserve the topological charge, even though one vortex has more energy than the other one. Furthermore, the scenario of the collision of opposite vortices described by isotropic Ginzburg-Landau (see Refs. [4,22] and references therein) does not account for the whole picture of the collision of opposite nematic umbilical defects as is shown in Ref. [23]. The characterization of vortex interaction in the anisotropic Ginzburg-Landau equation is in progress.

V. CONCLUSIONS AND REMARKS

The dissipative vortexlike defects, nematic umbilical, have accompanied liquid crystals since their discovery. In spite of the large amount of experimental and theoretical studies, an entire understanding of this phase singularity solutions has not been overtaken. The existence, stability properties, and bifurcation diagram of the nematic umbilical defects through amplitude equations was presented. Close to the Fréedericksz transition of a nematic liquid crystal with negative anisotropic dielectric constant and homeotropic anchoring, an anisotropic Ginzburg-Landau equation for the transversal critical mode, which is derived by taking the 3D to 2D limit of the Frank-Oseen model, is considered. This model is a variational generalization of the Ginzburg-Landau equation with real coefficients. This model allows us to reveal the mechanism of symmetry breaking of nematic umbilical defects. The defect with positive charge is fully characterized as a function of the anisotropy, while the negative defect is characterized perturbatively. In particular, only a discrete number of solutions of the continuous family of defect persist when anisotropy is considered. Numerical simulations show quite good agreement with the analytical results.

Recently, by sending circularly polarized light beams onto a homeotropic nematic liquid crystal cell with a photosensitive wall matter vortices were spontaneously induced that remain, each stable and trapped at the chosen location [26,27]. These optical lattices and others, like the ones created using magnets by Pieranski *et al.* [28] can be understood by this amplitude equation method. In particular we expect the positive vortex to rotate when the boundary or initial conditions do not agree with the phase jump imposed by the anisotropy, as is seen in Refs. [27,28].

The anisotropic Ginzburg-Landau equation opens new avenues to the study of nematic umbilical defects such as dynamical evolution and interaction.

ACKNOWLEDGMENTS

The authors thank C. Falcon for fruitful discussions. M.G.C., M.K., and J.D. thank the financial support of FONDECYT Projects No. 1120320, No. 1130126, and No. 1130360, respectively. E.V-H. thanks CONICYT-PCHA/Magíster Nacional/2013 - 221320023. M.K. and J.D. were partially supported by Fondo Basal CMM-Chile. Experimental image of umbilical defects [Fig. 1(c)] courtesy of V. Odent.

APPENDIX: 3D TO 2D ASYMPTOTICS FOR THE FULL FRANK-OSEEN MODEL NEAR THE FRÉEDERICKSZ TRANSITION

In this Appendix we provide some details of the calculation that leads from Eq. (1) to Eq. (2) in the limit $d \to 0$. As we pointed out it suffices to identify terms of order $\mathcal{O}(1)$ and those of order $\mathcal{O}(d^2)$. Taking into account that *a priori* $n_x = \mathcal{O}(d^2)$ and $n_y = \mathcal{O}(d^2)$ it is rather easy to identify these orders. For brevity in the following we will only consider the $\hat{x}$ component, calculations involving $\hat{y}$ component being similar. In the notation of Sec. II A we have the following terms at order $\mathcal{O}(1)$ and $\mathcal{O}(d^2)$:

$$\begin{aligned}-\big[&K_3\big(\nabla_\perp^2 n_x + d^{-2}\partial_{\zeta\zeta}^2 n_x - n_x n_z d^{-2}\partial_{\zeta\zeta}^2 n_z\big)\\&+(K_3-K_1)\big(n_x n_z d^{-2}\partial_{\zeta\zeta}^2 n_z - \partial_{xx}^2 n_x - \partial_{xy}^2 n_y\big)\\&-(K_2-K_3)\big(\partial_{xy}^2 n_y - \partial_{yy}^2 n_x\big)\big]\\&-\epsilon_a V_{FT}^2 d^{-2} n_x - 2\epsilon_a V_{FT} V_1 n_x + \gamma\,\partial_t n_x.\end{aligned}$$

Taking into account the definition of V_{FT} we see that $\mathcal{O}(1)$ terms above cancel and we are left with

$$\begin{aligned}g_x = -\big[&\big(K_1\partial_{xx}^2 u_0 + K_2\partial_{yy}^2 u_0 + (K_1-K_2)\partial_{xy}^2 v_0\big)\cos(\pi\zeta)\\&+K_1 u_0 \tfrac{1}{2}\big(u_0^2+v_0^2\big)\cos(\pi\zeta)\partial_{\zeta\zeta}^2\cos^2(\pi\zeta)\\&-2\epsilon_a V_{FT} V_1 u_0\cos(\pi\zeta)\big] + \gamma\cos(\pi\zeta)\partial_t u_0.\end{aligned}$$

Condition $\int_{-1/2}^{1/2} g_x\cos(\pi\zeta)\,d\zeta = 0$ leads to

$$\begin{aligned}\gamma\,\partial_t u_0 = &\frac{K_1+K_2}{2}\nabla_\perp^2 u_0\\&+\frac{K_1-K_2}{2}\big[\big(\partial_{xx}^2-\partial_{yy}^2\big)u_0 + 2\partial_{xy}^2 v_0\big]\\&-\frac{K_1}{2}\pi^2 u_0\big(u_0^2+v_0^2\big) - \epsilon_a V_{FT} V_1 u_0.\end{aligned}$$

From this, taking into account a similar equation in the direction $\hat{y}$ we get Eq. (2).

[1] G. Nicolis and I. Prigogine, *Self-Organization in Non-Equilibrium Systems* (Wiley, New York, 1977).
[2] L. M. Pismen, *Patterns and Interfaces in Dissipative Dynamics*, Springer Series in Synergetics (Springer, Berlin, 2006).
[3] M. C. Cross and P. C. Hohenberg, Rev. Mod. Phys. **65**, 851 (1993).
[4] L. M. Pismen, *Vortices in Nonlinear Fields* (Clarendon Press, Oxford, 1999), and references therein.
[5] S. Chandrasekhar, *Liquid Crystals* (Cambridge University Press, Cambridge, 1992).
[6] P. G. de Gennes and J. Prost, *The Physics of Liquid Crystals*, 2nd ed. (Oxford Science Publications, Clarendon Press, Oxford, 1993).
[7] P. Oswald and P. Pieranski, *Nematic and Cholesteric Liquid Crystals* (Taylor & Francis Group, Boca Raton, 2005).
[8] O. Lehmann, Z. Phys. Chem. **4**, 462 (1889).
[9] G. Friedel, Annales de Physique **18**, 273 (1922).
[10] F. C. Frank, Disc. Faraday Soc. **25**, 19 (1958).
[11] A. Rapini, J. Physique **34**, 629 (1973).
[12] T. Frisch, S. Rica, P. Coullet, and J. M. Gilli, Phys. Rev. Lett. **72**, 1471 (1994).
[13] T. Frisch, Physica D **84**, 601 (1995).
[14] A. Saupe, Mol. Cryst. Liq. Cryst. **21**, 211 (1973).
[15] I. S. Aranson and L. S. Tsimring, Phys. Rev. E **74**, 031915 (2006).
[16] I. Aranson and L. Kramer, Rev. Mod. Phys. **74**, 99 (2002).
[17] V. L. Ginzburg and L. P. Pitaevskii, Sov. Phys. JETP **7**, 858 (1958).
[18] F. Bethuel, H. Brezis, and F. Helein, *Ginzburg-Landau Vortices* (Springer, New York, 1994).
[19] Q. Han and T.-C. Lin, Nonlinearity **15**, 257 (2002).
[20] M. Kim and D. Phillips, Commun. Math. Phys. **310**, 299 (2012).
[21] R. B. Meyer, Philos. Mag. **27**, 405 (1973).
[22] R. Barboza, T. Sauma, U. Bortolozzo, G. Assanto, M. G. Clerc, and S. Residori, New J. Phys. **15**, 013028 (2013).
[23] I. Dierking, M. Ravnik, E. Lark, J. Healey, G. P. Alexander, and J. M. Yeomans, Phys. Rev. E **85**, 021703 (2012).
[24] S. H. Strogatz, *Nonlinear Dynamics and Chaos: With Applications to Physics, Biology, Chemistry and Engineering* (Addison-Wesley, Reading, Massachusetts, 1994).
[25] J. D. Crawford, Rev. Mod. Phys. **63**, 991 (1991).
[26] R. Barboza, U. Bortolozzo, G. Assanto, E. Vidal-Henriquez, M. G. Clerc, and S. Residori, Phys. Rev. Lett. **109**, 143901 (2012).
[27] R. Barboza, U. Bortolozzo, G. Assanto, E. Vidal-Henriquez, M. G. Clerc, and S. Residori, Phys. Rev. Lett. **111**, 093902 (2013).
[28] P. Pieranski, B. Yang, L. J. Burtz, A. Camu, and F. Simonetti, Liq. Cryst. **40**, 1593 (2013).